Electronic appendix: Analytical procedures, petrography and mineralogy

Includes the following tables:
Table ES-4: Petrography of the analysed samples
Table ES-5: Analyses of volcanic glasses
Table ES-6: Clinopyroxene analyses
Table ES-7: Amphibole analyses
Table ES-8: Biotite–phlogopite analyses
Table ES-9: Magnetite analyses

Analytical procedures for isotope analysis

For Nd - Sm isotopes, rock powders were accurately weighed and totally spiked with a known amount of mixed ^{150}Nd - ^{149}Sm tracer solution. Dissolution was carried out in 24N HF + 16N HNO_3 in sealed PFA Teflon vessels at 160°C for five days. The fluoride residue was converted to chloride with HCl, and Nd and Sm were separated by conventional cation and HDEHP-based chromatography. Chemical processing blanks were <40 picograms of either Sm or Nd, and are insignificant relative to the amount of Sm or Nd analysed for any rock sample. The isotopic composition of Nd was determined in static mode by Multi-Collector ICP-Mass Spectrometry. All isotope ratios were normalized for variable mass fractionation to a value of ^{146}Nd/^{144}Nd = 0.7219 using the exponential fractionation law. The ^{143}Nd/^{144}Nd ratio of samples is presented relative to a value of 0.511850 for the La Jolla Nd isotopic standard, monitored by use of an Alfa Nd isotopic standard for each analytical session. Sm isotopic abundances were measured in static mode by Thermal Ionization Mass Spectrometry, and are normalized for variable mass fractionation to a value of 1.17537 for ^{152}Sm/^{154}Sm also using the exponential law. The mixed ^{150}Nd-^{159}Sm tracer solution used was calibrated directly against the Caltech mixed Sm/Nd normal described by Wasserburg et al. (1981). Using this mixed tracer, the measured ^{147}Sm/^{144}Nd ratios for the international rock standard BCR-1 range from 0.1380 to 0.1382, suggesting a reproducibility for ^{147}Sm/^{144}Nd of about ± 0.1% for real rock powders. The value of ^{147}Sm/^{144}Nd determined for BCR-1 is within the range of reported literature values by isotope dilution methods. The error on Sm/Nd ratio was monitored and controlled through the ^{147}Sm/^{144}Nd ratio, with a Sm/Nd isotopic analyses of the BCR-1 international rock standard carried out on a regular basis using the same procedure as described above. Based on a large number of measurements over the past few years, the reproducibility of its ^{147}Sm/^{144}Nd ratio is ± 0.1% at 1 sigma error level.

Sr isotopic compositions were determined on a separate powder aliquot using the same dissolution procedures as for Sm-Nd analysis. No isotopic tracer was used in this procedure. Sr was separated using standard cation exchange chromatography, with Sr blanks of < 200 pg Sr.

Isotopic compositions were determined by TIMS and presented relative to a value of 0.710245 for the NIST SRM987 Sr isotope standard.

Petrography

Northern part of the Katalakon Unit

Hyabyssal intrusive sheets sampled in the northwestern portion of the island near the stock or dome of Skalosies (samples LM02, 03, 04) are petrographically similar to the dacite sampled at the edge of the stock (LM06) (Table ES-4). These rocks are highly porphyritic and are characterized by phenocrysts and microphenocrysts of feldspar, idiomorphic amphibole ± biotite, set in a greenish-brown groundmass comprised of a very fine grained intergrowth of feldspars, dusty opaques and devitrified glass, partially altered to chlorite. Some samples may also contain pyroxene phenocrysts, however, a positive identification is not possible due to the pervasive alteration to chlorite + calcite + opaques ± sericite, and the lack of characteristic basal sections by which a more definitive identification could be made. The dyke rocks sampled in this locality are spherulitic and commonly also contain small cavities filled with calcite and apatite; small spherules containing quartz ± calcite ± chlorite ± epidote are found in the dacite sampled from the stock (LM06). All of the rocks sampled in this locality are highly altered, to the extent that most minerals have been identified primarily on the basis of crystal form and discrimination between plagioclase and K-feldspar was not possible. Feldspar laths are entirely altered to a mixture of very fine-grained clays ± calcite; some phenocrysts are slightly embayed. Amphibole and biotite grains are often entirely altered to opaques + chlorite ± calcite ± actinolite ± muscovite ± sericite ± epidote, however idiomorphic crystal outlines have been preserved. Common accessory mineral phases are apatite, zircon, magnetite and titanomagnetite.

Samples from near the village of Katalakon are mostly dykes, with lesser sills and stocks (samples LM35, 39, 40, 41, 42, 43). These rocks are mostly dacites, with one andesite dyke (LM42). Biotite is present more consistently in these rocks and pyroxene is confirmed in a few samples, although still identified on the basis of crystal outline. Zoning is present in most plagioclase phenocrysts, and has been observed in rare amphibole grains. Most of these samples are either spherulitic or have only small spherules containing quartz ± calcite; one sample contains a small cavity lined with quartz at the rim and filled in with calcite. Alteration is not as extensive in all of these samples as it is in the dyke rocks near Skalosies, however several samples are quite heavily altered and there is a more variable character to the alteration observed in these rocks. Samples LM41 and LM42 more closely resemble the dyke rocks sampled near Skalosies, but show a more definite presence of pyroxene occurring as phenocrysts in minor amounts; both samples are heavily altered, although LM41 has more iron-rich alteration products disseminated throughout the rock. Samples LM39 and LM40 have similar mineralogy and are particularly abundant in hydrous phases, especially in comparison to sample LM43, and LM35 to a lesser degree; LM39 shows extensive pyritization. In the less altered rocks, amphibole and biotite grains are variably altered to opaques, ranging from only thin opacitic rims to entirely altered crystals. In the more heavily altered samples, alteration products are the same as those listed above; sample LM35 shows clinopyroxene phenocrysts almost entirely replaced by epidote. Accessory mineral phases include apatite, zircon, sphene, allanite (present in only one sample), magnetite and titanomagnetite.

Fakos quartz monzonite

Rocks from the Fakos quartz monzonite (LM45, 48, 50) are characterized by relatively consistent mineralogy although samples LM45 and LM50 are porphyritic rocks, while LM48 is comprised of medium-grained interlocking crystals. LM45 and LM50 are characterized by phenocrysts and microphenocrysts of plagioclase, ?K-feldspar (alteration makes identification difficult), clinopyroxene, biotite ± quartz, set in a hyalopilitic groundmass. LM48 is a medium-grained, holocrystalline rock with inequigranular, interlocking crystals; major minerals are plagioclase, K-feldspar, and quartz, with subordinate brown-green amphibole and biotite. Primary amphibole is only present in LM48; in the two other samples, clinopyroxene is variably altered to actinolite (pervasively in LM45, less extensively in LM50). Other alteration products include epidote, chlorite, calcite, and opaque oxides. Accessory mineral phases include apatite, zircon, sphene, magnetite and titanomagnetite.

Southern part of the Katalakon Unit

Sample LM72 is a highly porphyritic trachyandesite and shares similar mineralogy to the northern Katalakon Unit rocks described above, but with the following exceptions: in LM72, biotite is more abundant than amphibole, there are fewer phenocrysts and microphenocrysts present, the groundmass is darker in colour and even finer grained (although still hyalopilitic), and the rock is not spherulitic, although small cavities filled with calcite + quartz do exist. Also, the degree of alteration in LM72 is considerably less advanced; feldspars and biotite are unaltered, however, amphibole grains are entirely replaced by chlorite + calcite + opaques. There is no evidence of pyroxene in LM72.

Romanou Unit

(1) Rhyolite, as lava dome (LM27) and lava breccia (LM22) has phenocrysts and microphenocrysts of plagioclase, K-feldspar (?sanidine), biotite, ± rare amphibole ± rare pyroxene in a groundmass of altered glass. K-feldspar phenocrysts are typically rounded but

otherwise unaltered while plagioclase phenocrysts are both embayed and somewhat altered; the ferromagnesian minerals are heavily altered and have been identified on the basis of crystal form. (2) Trachydacites as a lava flow (LM24) and as an intrusion or enclave in the rhyolite lava dome (LM25) contain phenocrysts and microphenocrysts of plagioclase (infrequently zoned), clinopyroxene, biotite, amphibole and rare K-feldspar, set in a groundmass of microlites of the same minerals surrounded by devitrified glass; small patches of altered brown glass are also commonly found dispersed in the groundmass of the rock. Feldspar phenocrysts are commonly embayed, while clinopyroxene, biotite, and amphibole typically occur as idiomorphic grains, but are variably altered to opaques, chlorite, and a mixture of clays. One sample from this group contains a cognate enclave comprised of intergrown feldspar laths, elongated biotite crystals with rare clinopyroxene grains and interstitial brown glass. Zircon, magnetite, and titanomagnetite are present as accessory mineral phases.

(3) Clasts from breccias and conglomerates (LM28, 30, 31, 32) are trachyandesites. The rocks in this group are very consistent in their mineralogy and are characterized by phenocrysts and microphenocrysts of clinopyroxene, subordinate plagioclase and biotite, ± rare K-feldspar, set in a hyalopilitic groundmass. In some samples the groundmass appears to be predominantly dusty brown glass with a lesser amount of microcrystalline. Zoning is common in both clinopyroxene and plagioclase phenocrysts, the latter of which is typically embayed. Several cognate enclaves have been found in these rocks, some of which are present in more than one sample. The enclaves are very fine-grained aggregates of the same minerals present in the rock, occurring as granular masses of plagioclase + clinopyroxene + biotite + opaques, and as (smaller) masses of biotite + plagioclase + opaques. Alteration in these rocks is overall very minimal: biotite in LM28 is variably altered to opaques, ranging from moderately thick opacitic rims to crystals entirely replaced by opaques, but in all other samples, only some phenocrysts of biotite appear altered ("baked"), while the majority of biotite grains remain unaltered (as are the other minerals present in the rock). Apatite, zircon, magnetite, and titanomagnetite are present as accessory minerals in these rocks.

(4) Trachydacites from the Romanou Unit in the southwest occur as a lava (LM65) and a block in a polymictic breccia (LM66). They contain variable amounts of clinopyroxene (most commonly as microphenocrysts), have small patches of altered brown glass dispersed throughout the rock. LM65 has comparatively fewer plagioclase phenocrysts (still occurring typically as cumulophyric aggregates) but also has abundant microphenocrysts of pyroxene (now entirely replaced), similar to LM66. Biotite is again more abundant than amphibole, the latter of which is typically more altered to opaque oxides, but with variable degrees of alteration in both minerals. The groundmass in LM65 is somewhat more glassy, with small patches of altered brown glass

dispersed throughout the rock as well as some portions of groundmass that appear to be predominantly dusty glass.

Agios Ioannis sub-unit

The trachydacite (LM07, 11, 13, 15) from the Agios Ioannis subunit is comprised of highly porphyritic rocks characterized by phenocrysts of plagioclase, with subordinate biotite, amphibole, K-feldspar and quartz, with microphenocrysts of predominantly idiomorphic amphibole ± biotite, and subordinate feldspar, set in a hyalopilitic groundmass. Plagioclase phenocrysts commonly occur as cumulophyric aggregates; sample LM13 contains glomerophyric clots of plagioclase ± interstitial glass. Zoning in plagioclase phenocrysts is common, but variable between samples; occasional feldspar phenocrysts have idiomorphic overgrowths on subhedral cores. Sample LM11 is hydrothermally altered to quartz + chlorite + sericite + opaques, but preserves crystal outlines of pyroxene. Alteration in the other rocks is of moderate intensity; plagioclase, quartz and K-feldspar phenocrysts are commonly embayed, and hydrous phases are variably altered to opaques. Biotite is typically less altered than amphibole, the latter of which is frequently altered entirely to opaques while relatively unaltered biotite grains coexist in the same sample; most commonly, however, both minerals show a range of alteration within each sample, varying from only thin opacitic rims to entire replacement of the original crystal. Other alteration products include calcite, chlorite, hematite, and sericite. Small spherules containing quartz ± calcite ± chlorite are present in these rocks. Common accessory mineral phases are apatite, zircon, sphene, magnetite and titanomagnetite.

Sample LM14 is rhyolitic dyke rock. It is weakly porphyritic and contains fragmented crystals of plagioclase, K-feldspar, amphibole, biotite, and quartz, set in a light brown groundmass consisting of a very fine-grained dusty intergrowth of the same minerals plus opaques. Alteration is moderate and is most pronounced in hydrous phases: many amphibole crystals are altered and have opacitic rims of variable thicknesses; biotite crystals are commonly kinked as a result of lava flow but usually have only thin opacitic rims. Plagioclase phenocrysts are typically fractured and embayed. Apatite, zircon, ?tourmaline, and magnetite occur as accessory minerals.

Myrina Unit

Porphyritic rocks sampled from a foliated dome (LM53, 57, 58) form a distinctive group of trachydacites characterized by phenocrysts of plagioclase, K-feldspar, rare biotite, amphibole ± quartz, with abundant microphenocrysts of feldspars and rare biotite, set in a hyalopilitic to trachytic (LM53) groundmass. Most feldspar phenocrysts have idiomorphic overgrowths around subhedral cores; in some grains, a thick band of sieve texture separates the overgrowth from the core, while in others such alteration is entirely absent. Biotite phenocrysts are moderately to heavily altered to opaques; amphibole grains are commonly heavily altered to opaques + chlorite ± calcite. Other alteration products include hematite and epidote. Small spherules of quartz ± chlorite ± calcite ± opaques are present in all three samples. Accessory mineral phases include apatite, zircon, and magnetite.

A second group of trachydacites from the Myrina Unit (LM 61, 64) are petrographically similar to the first group but have more groundmass glass and LM61 has rare microphenocrysts of clinopyroxene. Biotite is typically much more abundant and far less altered than amphibole in these rocks.

Chemical mineralogy

Feldspars

The majority of plagioclase in the Limnos volcanic rocks is andesine, with minor labradorite and oligoclase, and rare albite; sanidine is also present in some of the samples (Fig. 9a, 10a). Compositional varations and differences in the zoning patterns of feldspar grains between the different units is discussed below.

Katalakon Unit – Feldspar grains analyzed from LM72, LM40, and LM43 all have the composition of andesine, with only few labradorite core and inner rim compositions. Phenocrysts show complex, but in general, normal zoning patterns, with anorthite contents ranging from An_{52} in some cores to An_{30} in the outermost rims. However, oscillatory zoning with An_{50} close to the rim is seen in at least one sample. Microphenocrysts analyzed have An_{34-48}, and thus show a range in compositions that agree with both cores and rims of phenocrysts.

Agios Ioannis sub-unit – LM13 contains phenocrysts of andesine with reversely zoned cores and rims (An_{30} to An_{46} in the core, and An_{32} to An_{40} in the rim), normally zoned cores (An_{37} to An_{30}) with thin but more calcic rims (An_{40}), and also reversely zoned cores (An_{29} to An_{32}) with normally zoned rims (An_{47} to An_{37}); LM15 and LM07 contain phenocrysts with complex oscillatory zoning patterns. Microphenocrysts in LM13 and LM15 generally agree with phenocryst rim compositions within each sample.

Fakos quartz monzonite – Plagioclase grains analyzed are predominantly andesines with minor albite. Andesine phenocrysts show normal or oscillatory zoning patterns. Some microphenocrysts showed reverse zoning, with a core of An_{32} and a rim of An_{43}, however, other microphenocrysts have the composition of secondary albite.

Romanou Unit –Most analyzed plagioclase grains have the composition of andesine, with few phenocryst rims of labradoritic composition; potassic feldspars plot in the sanidine field. Considerable variability exists in the zoning patterns of feldspars within this unit. Some plagioclase phenocrysts in LM31 have thin, more calcic rims (An_{54}) around subhedral cores (An_{41}). In LM32, reverse zoning is present in the core (An_{38} to An_{40}), but normal zoning in the rim (An_{50} to An_{38}). LM24 has phenocrysts of normally zoned andesine cores (An_{40} to An_{32}) with potassic overgrowths (Or_{58} to Or_{56}). In both LM25 and LM22, plagioclase phenocrysts show oscillatory zoning with an overall normal zoning trend. Sanidine phenocrysts are present in LM22 and microlites in the groundmass of LM22 have the composition of sanidine. Microphenocrysts analyzed in LM25 agree with the composition of phenocrysts rims (~An_{36}). LM65B has normally zoned phenocrysts that show anorthite contents gradually decreasing from An_{41} in the core to An_{27} in the rim.

Myrina Unit –Feldspars in the Myrina Unit show a wider compositional range as compared to the other Limnos volcanic units. Phenocryst compositions range from labradorite to oligoclase in the Ab-An series, however, sanidine phenocrysts are present as well. Zoning patterns in plagioclase phenocrysts are quite varied: LM58 shows normally zoned slightly subhedral cores (An_{48} to An_{43}) with normally zoned euhedral overgrowths (An_{59} to An_{54}); and LM61 contains both phenocrysts with normally zoned cores (An_{37} to An_{23}) and reversely zoned rims (An_{28} to An_{33}), in addition to phenocrysts with reversely zoned cores (An_{45} to An_{61}) and normally zoned rims (An_{29} to An_{26}). Microphenocrysts in LM58 generally agree with phenocryst rim compositions. In LM61, an analyzed calcic microphenocryst (An_{51}) has a composition similar to the center of a reversely zoned core (An_{45} to An_{61}) which is surrounded by a normally zoned and much more albitic rim (An_{29} to An_{26}).

Pyroxenes

Samples from the Romanou, Myrina, and Fakos units show little overall compositional variation as all analyzed grains plot close to the boundary between augite and diopside (Fig. 10). Orthopyroxene was not found in any of the samples.

Normal zoning in clinopyroxene phenocrysts and microphenocrysts is pervasive in samples from both the Romanou and Fakos units. Crystals commonly display repetitive gradations from a more primitive to a more evolved composition, with each more primitive zone preceded by a corrosion event. In some cases, as many as three such oscillatory zoning cycles are present. Phenocrysts from LM31 and LM32 in the Romanou Unit, and LM50 and LM45 in the Fakos quartz monzonite, display very similar zoning patterns: both the core (analyses a and b) and the rim (analyses c and d) show a normal zoning pattern, however, the onset of the second compositional band is comparatively enriched in Cr_2O_3 and MgO and relatively depleted in FeO with respect to the core, including the very center of the core in some cases. Rare clinopyroxene microphenocrysts in the Myrina Unit are similar in composition to the more primitive compositions obtained for the innermost portion of phenocryst rims ("c" analyses) in the Romanou and Fakos units.

Amphiboles

Amphibole phenocrysts and microphenocrysts from the Katalakon and Myrina units (including the Agios Ioannis sub-unit) are calcic amphiboles. The Myrina Unit is characterized by magnesio-hornblende, edenite-hornblende, and magnesio-hastingsite; the Agios Ioannis sub-unit by edenite, magnesian hastingsite and edenitic hornblende, while the Katalakon Unit is restricted to primarily magnesio-hastingsitic hornblende and magnesian hastingsitic-hornblende (Fig. 10). All of the grains have similar Mg/(Mg+Fe^{2+}) ratios, but occupy different ranges of Si in relation to them: the Myrina and Agios Ioannis amphiboles encompass a slightly broader range of Si, with values above and below those for the Katalakon amphiboles, but not overlapping.

Oscillatory zoning is present in some amphiboles from the Katalakon Unit, however, the extensive alteration of amphiboles in many of the samples from the various units makes it impossible to determine if this is a common trend. An amphibole phenocryst from sample LM43 in the Katalakon Unit shows reverse zoning in the core surrounded by a rim of fairly constant (and more evolved) composition; the outer rim of the phenocryst is quite corroded. Repetitive oscillatory zoning is present in an amphibole phenocryst from LM40 (also Katalakon Unit) with at least two corrosion events and at least three euhedral growth phases rich in inclusions. A microphenocryst has a composition similar to the outermost rim of the phenocryst. Normal zoning is present in an amphibole phenocryst from LM61 in the Myrina Unit. Other amphibole phenocrysts have relatively uniform composition throughout the grain, from the center of the core to the rim, or from the outer core to the rim.

Biotite

Biotite grains in the Limnos volcanic rocks are fairly consistent in their composition and lack apparent distinction between the various units; however, some subtle differences do exist in the relative abundances of particular chemical constituents between grains from different units. The analyses of selected grains plot in the phlogopite-annite series, but overall tend to be more Mg-rich. TiO_2 contents range from 4.2 to 7.1 wt.%; the lowest values are associated with the Myrina Unit, the Katalakon Unit is intermediate in range, and the highest values are found in the Fakos and Romanou units. Higher NiO values (above 0.5 wt.%, ranging up to 1.75 wt.%) are also associated primarily with the Romanou Unit, while negligible amounts are found in most of the Myrina and Katalakon biotite grains analyzed.

Alteration products

Many of the studied rocks are moderately to extensively altered and some chemical analyses have been used to confirm the optical identification of the various alteration products observed in these rocks. Alteration products include chlorite, sericite, calcite, actinolite, epidote, albite, and barite; fine-grained mixtures of clay minerals are difficult to identify precisely but are present as alteration products in several samples as well.

Accessory minerals

Optical identification of accessory mineral phases was confirmed using primarily an energy dispersive system (EDS) in conjunction with some wavelength-dispersive (WDS) electron-microprobe analyses. Common accessory minerals include apatite, zircon, sphene, magnetite and titano-magnetite (magnetite analyses are given in Table ES-9). Allanite has been found in LM40 and monazite in LM72.

References

Wasserburg, G.J., Jacobsen, S.B., DePaolo, D.J., McCulloch, M.T., and Wen, T., 1981, Precise determination of Sm/Nd ratios, Sm and Nd isotopic abundances in standard solutions: Geochimica et Cosmochimica Acta, v. 45, p. 2311–2323.

Table 4 Petrographical characteristics of analysed samples

Sample	Latititude	Longitude	Unit[1]	Field Occurrence	Rock Name[2]	Texture	Degree of alteration[3]	Phenocrysts & microphenocrysts[4]	Groundmass	Remarks, alteration products
LM02	39.96	25.11	KN	sill, 20 cm from top	dacite	porphyritic; spherulitic	high	feld$^+$; idiom amph$^+$; ?bi; ?px	hyalopilitic	Alt: cc; op; chl; act; ser; ms. Cavities filled with cc+ap.
LM06	39.97	25.08	KN	stock (intrusion)	trachyte	porphyritic	high	feld$^+$; amph$^+$; ?bi	hyalopilitic	Alt: cc; op; chl; act; ser; ms; ep. Small spherules of qtz±cc±chl±ep.
LM07	39.94	25.05	AI	?	trachydacite	porphyritic	med	plag; bi$^+$; idiom amph$^+$; K-feld; qtz	hyalopilitic	Alt: op; chl; hem; ?ep. Plag mgxt with growth twins; plag+qtz ph embayed; Spherules of qtz±chl.
LM11	39.93	25.06	AI	?	trachyte	porphyritic	high	plag; amph$^+$; bi; K-feld; qtz; ?px	hyalopilitic	Hydrothermal alt: chl; op; ser. Qtz ph embayed. Amph±?px replaced by qtz+chl+ser+op.
LM13	39.92	25.07	AI	?lava dome	trachyandesite	porphyritic	med	plag; idiom amph; bi; K-feld	hyalopilitic	Alt: cc; op; chl. Bi ph show flow texture. Plag ph embayed; some plag ph with idiom overgrowths. Cognate enclave of amph+plag+op. Small spherules of qtz±chl and cc veinlets. Glomerophyric clots of plag± interstitial glass.
LM14	39.92	25.07	AI	dyke in dacite	rhyolite	porphyritic	med	plag; K-feld; qtz; amph; bi;	hyalopilitic	Alt: op. Few bi ph show flow texture. Plag, qtz, K-feld ph fragmented and embayed.
LM15	39.92	25.14	AI	?	trachyte	porphyritic	med	plag; idiom bi; idiom amph; K-feld; rare qtz	hyalopilitic	Alt: op; chl. Spherules of qtz. Qtz ph rounded.
LM18	39.85	25.32	R	lava breccia	trachyte	porphyritic	high	plag; K-feld; px; biotite; amph	hyalopilitic	Alt: amph, biotite, and px altering to op. Plagioclase altering to chl.
LM24	39.88	25.31	R	lava	trachyte	porphyritic	med	plag; idiom px$^+$; bi$^+$; amph$^+$; rare K-feld	hyalopilitic w/ small patches alt brn glass	Alt: op; chl; clays.
LM25	39.88	25.31	R	intrusion in ?lava dome	trachyte	porphyritic	med	plag; idiom cpx; idiom bi; idiom amph; rare K-feld	hyalopilitic w/ small patches alt brn glass	Alt: op; chl; clays; ser. Cognate enclaves of feld+bi+cpx+interstitial glass.
LM28	39.91	25.29	R	lava breccia	trachyandesite	porphyritic	low	cpx; plag; bi; K-feld	hyalopilitic	Alt: op. Plag ph embayed. Zoning in cpx common. Cognate enclaves of cpx+plag+bi+op.
LM30	39.92	25.3	R	clast in conglomerate	trachyandesite	porphyritic	low	cpx; plag; bi; rare K-feld	hyalopilitic; largely dusty brown glass	Plag ph embayed. Zoning in cpx common. Cognate enclave of cpx+op+bi+plag.
LM31	39.92	25.3	R	clast in conglomerate	trachyandesite	porphyritic	low	cpx; plag; bi; rare K-feld	hyalopilitic; largely dusty brown glass	Plag ph embayed. Zoning in cpx common. Cognate enclaves of plag+cpx+bi+op and bi+plag+op.
LM32	39.92	25.3	R	clast in conglomerate	trachyandesite	porphyritic	low	cpx; plag; bi	hyalopilitic; largely dusty brown glass	Plag ph embayed. Zoning in cpx common.
LM35	39.94	25.15	KN	?lava	dacite	porphyritic	high	plag; ?px; ?amph; ?K-feld	hyalopilitic	Alt: chl; ep; op; ser.
LM39	39.95	25.16	KN	?lava	dacite	porphyritic; spherulitic	high	plag; bi; idiom amph$^+$	hyalopilitic	Alt: hem; op; chl; act; ep; clays. Spherules containing qtz (+spherulites).
LM40	39.95	25.17	KN	dyke	dacite	porphyritic; spherulitic	low	plag; idiom amph; bi	hyalopilitic	Alt: op; clays. Bi ph show flow texture. Plag ph embayed. Small cavities filled with qtz+ap; 3 crystals idiom allanite.
LM41	39.95	39.95	KN	?stock (intrusion)	dacite	porphyritic	high	feld$^+$; idiom amph$^+$; px$^+$; bi$^+$	hyalopilitic	Alt: cc; chl; op; ser; ep; clays. Spherules of qtz.
LM43	39.96	25.16	KN	dyke	dacite	porphyritic	med	plag; amph; bi	hyalopilitic	Alt: op; cc; ser; clays. Plag ph embayed. Very small spherules of qtz.
LM44	39.94	25.14	KN	float of intrusion	dacite	porphyritic	med	plag; K-feld; amph; biotite	hyalopilitic	Alt: amph altering to op.
LM45	39.81	25.17	F	(intrusion)	trachyte	porphyritic	high	plag; ?K-feld; cpx; bi	hyalopilitic	Alt: op; chl; cc; act; ep. Plag ph embayed. Cavities containing ep±act±chl±qtz. Cognate enclave of cpx+chl+act+ep+op.
LM48	39.82	25.17	F	dyke	trachyte	interlocking crystals	med	major minerals: plag; K-feld; qtz; amph; cpx; bi	N/A	Alt: chl; op. Medium-grained, inequigranular, interlocking texture.
LM50	39.82	25.17	F	dyke	trachyandesite	porphyritic	med	idiom cpx; plag; bi; rare qtz	hyalopilitic	Plag+qtz ph embayed. Cognate enclaves of cpx(alt)+plag+qtz+op and bi+op+plag.
LM53	39.92	25.08	M	lava dome	trachydacite	porphyritic	med	plag; K-feld; bi; rare idiom amph	trachytic	Alt: op; cc; chl; ep. Spherules of qtz+chl±cc. Idiom overgrowths of feld on subhedral plag; also plag ph embayed. Cognate enclave of plag+op+chl+cc.
LM54	39.92	25.08	M	lava dome	trachyte	porphyritic	high	plag; K-feld; qtz; biotite	trachytic	Alt: plag altering to cc. Biotite altering to op.
LM57	39.92	25.08	M	lava dome	trachydacite	porphyritic	med	plag; K-feld; bi; rare qtz; ?amph	hyalopilitic	Alt: hem; op; clays. Spherules of qtz±op±chl. Qtz ph embayed. Vein of dusty vfn qtz+glass+op. Idiom feld overgrowths on subhedral plag laths.

Table 4 Petrographical characteristics of analysed samples

Sample	Latititude	Longitude	Unit[1]	Field Occurrence	Rock Name[2]	Texture	Degree of alteration[3]	Phenocrysts & microphenocrysts[4]	Groundmass	Remarks, alteration products
LM58	39.92	25.08	M	lava dome	trachyte	porphyritic	med	plag; K-feld; bi; ?amph;	hyalopilitic	Alt: op; cc; chl; clays. Spherules of qtz+chl±cc. Idiom plag overgrowths on plag phenocrysts (subhedral to idiom).
LM61	39.85	25.07	M	lava flow	trachydacite	porphyritic	med	plag; qtz; idiom amph; bi; rare cpx	hyalopilitic w/ small patches alt brn glass	Alt: op. Glass incl in plag ph; cumulophyric plag. Qtz is rounded and embayed.
LM64	39.85	25.07	M	?lava dome	trachyte	porphyritic	med	plag; bi; idiom amph; qtz	hyalopilitic w/ small patches alt brn glass	Alt: op. Few idiom cpx mph. Qtz+plag ph embayed. Few zoned amph grains.
LM66	39.86	25.17	R	block in polymictic breccia	trachyte	porphyritic	med	plag; bi; idiom amph+; qtz; cpx, K-feld	hyalopilitic	Alt: op. Plag commonly embayed.
LM69	39.86	25.17	KS	lava	andesite	porphyritic	high	plag; cpx; biotite; amph	hyalopilitic	Alt: plag altering to cc. Biotite altering to op.
LM70B	39.87	25.18	R	lava breccia	trachyandesite	porphyritic	med	plag; biotite	hyalopilitic	Alt: biotite slightly altering to op.
LM72	39.9	25.17	KS	margin of dyke or stock	trachyandesite	porphyritic	med	plag; bi; idiom amph+; K-feld; qtz	hyalopilitic	Alt: op; cc; chl. Plag+qtz ph embayed. Cognate enclave of bi+amph(alt)+op+ glass. Small cavities filled with cc±qtz.
LM77	39.85	25.07	M	mxtic lava breccia	trachyte	porphyritic	high	K-feld; plag; amph; biotite	hyalopilitic	Alt: biotite and amph altering to op.
LM85	39.88	25.27	KS	lava dome	trachyandesite	porphyritic	med	plag; biotite; qtz; biotite	hyalopilitic	Alt: amph altering to cc and op. Biotite altering to cc and clay minerals.

[1]AI = Agios Ioannis; F = Fakos; M = Myrina; KN = Katalakon (north); KS = Katalakon (south); R = Romanou; [2]Rock nomenclature according to IUGS classification system (LeBas et al., 1986).
[3]Degree of alteration is a comparative assessmentof alteration in the studied rocks; [4]Phenocrysts and microphenocrysts are listed in order of decreasing abundance; +identified by crystal habit and form;
Abbreviations: act, actinolite; alt, altered/alteration; amph, amphibole; ap, apatite; bi, biotite; brn, brown; cc, calcite; chl, chlorite; cpx, clinopyroxene; ep, epidote; feld, feldspar; hem, hematite; idiom, idiomorphic; incl, inclusion; K-feld, K-feldspar; mgxt, megacryst; mph, microphenocryst; ms, muscovite; op, opaque oxide minerals; ph, phenocryst; plag, plagioclase; px, pyroxene; qtz, quartz; ser, sericite; sm, small; vfn, very fine-grained.

Table 5: Electron microprobe analyses of volcanic glasses

Rock Type[1]	Tra		Raft in Ignimbrite									
Sample	LM32-105	LM32-106	LM33-1	LM33-2	LM33-3	LM33-4	LM33-5	LM33-6	LM33-7	LM33-8	LM33-9	LM33-10
Major element oxides and select trace elements (wt %)												
SiO_2	68.57	69.31	64.83	65.46	65.10	64.93	65.10	65.43	65.40	64.70	64.89	65.19
TiO_2	0.64	0.61	0.29	0.30	0.33	0.34	0.32	0.36	0.34	0.35	0.32	0.34
Al_2O_3	14.54	14.38	14.69	14.56	14.71	14.44	14.80	14.84	14.81	14.62	14.57	14.56
FeO_t	2.36	2.33	1.76	1.46	1.57	1.77	1.63	1.06	1.14	1.95	2.15	1.55
MnO	0.21	0.22	0.04	0	0.02	0.04	0.04	b.d.	0.02	0.05	0.02	0.01
MgO	0.58	0.59	0.52	0.32	0.47	0.54	0.58	0.45	0.40	0.50	0.43	0.44
CaO	1.36	1.39	1.89	1.29	1.80	1.63	1.86	1.66	1.54	1.58	1.57	1.54
Na_2O	1.64	1.48	2.48	2.58	2.30	2.33	3.00	2.49	2.93	2.65	3.05	3.21
K_2O	6.83	6.91	7.65	6.52	7.50	7.48	6.74	7.41	6.85	6.96	6.71	7.00
P_2O_5	0.13	0.12	b.d.	b.d.	b.d.	b.d.	b.d.	b.d.	b.d.	b.d.	b.d.	b.d.
BaO	0.20	0.22	0.24	0.21	0.18	0.19	0.23	0.22	0.21	0.17	0.20	0.19
SrO	b.d.[2]	b.d.	0.12	0.10	0.10	0.14	0.09	0.04	0.08	0.10	0.11	0.14
Cl	b.d.	b.d.	0.11	0.10	0.06	0.06	0.10	0.11	0.11	0.11	0.09	0.13
Total	97.06	97.56	94.63	92.91	94.14	93.86	94.49	94.07	93.84	93.74	94.13	94.30
Rock Type	IgnR	Trd	Ignimbrite									
Sample	LM33-12	LM61-107	LM84-1	LM84-2	LM84-3	LM84-4	LM84-5	LM84-7	LM84-8	LM84-9	LM84-10	LM84-11
Major element oxides and select trace elements (wt %)												
SiO_2	65.70	67.91	66.96	65.47	66.36	67.20	67.11	66.90	66.78	65.54	66.65	67.16
TiO_2	0.31	b.d.	0.34	0.30	0.31	0.31	0.34	0.33	0.23	0.30	0.30	0.33
Al_2O_3	14.71	16.93	15.53	15.31	15.68	15.28	15.59	15.69	15.53	15.19	15.28	15.13
FeO_t	1.47	0.46	0.98	1.93	1.18	0.60	0.87	0.39	0.53	1.88	0.44	0.30
MnO	0.04	b.d.	0.03	0.05	0.05	0.05	0.04	0.02	0.03	0.06	0.01	0.03
MgO	0.35	b.d.	0.38	0.51	0.29	0.14	0.15	0.05	0.15	0.48	0.08	0.01
CaO	1.32	0.12	1.24	1.69	1.12	0.68	0.68	0.71	0.81	1.77	0.67	0.59
Na_2O	3.46	3.20	3.24	2.90	2.42	2.55	2.50	2.17	2.45	2.51	2.21	3.18
K_2O	6.80	11.19	6.91	6.93	7.08	7.46	7.58	7.45	7.37	6.97	7.60	7.46
P_2O_5	b.d.	b.d.	b.d.	b.d.	b.d.	b.d.	b.d.	b.d.	b.d.	b.d.	b.d.	b.d.
BaO	0.15	b.d.	0.21	0.09	0.22	0.13	0.16	0.19	0.18	0.22	0.27	0.20
SrO	0.06	b.d.	0.03	0.01	0.03	0.02	0.05	0.05	0.05	0.06	0.12	0.11
Cl	0.12	b.d.	0.06	0.05	0.10	0.11	0.09	0.10	0.10	0.10	0.11	0.10
Total	94.48	99.81	95.91	95.24	94.85	94.53	95.15	94.05	94.22	95.09	93.75	94.61

[1] Tra = trachyandesite clast in conglomerate (glass from a mineral clot); IgnR = raft in ignimbrite; Trd = trachydacite glass inclusion in plagioclase

[2] b.d. = below detection limit

Table 6 Electron microprobe analyses of clinopyroxene grains from selected samples of representative volcanic rocks.

Unit[1]	Romanou											
Sample	LM31	LM31	LM31	LM31	LM31	LM31	LM31	LM31	LM31	LM31	LM31	LM31
Analysis no.*	40a+	40b+	40c+	40d+	42a+	42b+	42c+	42d+	43a	43b	43c	43d
SiO_2	53.54	52.20	54.02	53.15	53.19	52.80	54.87	51.82	53.98	52.94	54.12	53.01
TiO_2	0.40	0.60	0.49	0.32	0.30	0.34	0.18	0.62	0.06	0.31	0.27	0.34
Al_2O_3	1.59	2.65	1.40	1.47	1.44	1.97	1.20	2.89	1.80	1.60	1.39	1.63
Cr_2O_3	0.01	0.03	0.04	0.03	0.03	0.01	0.60	b.d.	0.06	0.02	0.81	0.02
FeO_t	7.06	7.80	4.78	8.17	8.42	9.12	4.69	8.28	6.24	8.94	4.22	7.72
MnO	0.29	0.33	0.14	0.53	0.53	0.49	0.15	0.35	0.34	0.50	0.14	0.43
MgO	16.05	14.85	17.22	15.44	14.78	14.21	19.73	15.70	15.81	14.68	18.13	15.78
CaO	22.38	22.49	23.28	21.61	22.21	21.81	19.84	21.05	23.17	21.73	21.98	21.32
Na_2O	0.40	0.54	0.25	0.54	0.55	0.69	0.29	0.45	0.47	0.65	0.33	0.43
Total^	101.72	101.49	101.63	101.26	101.45	101.43	101.56	101.15	101.93	101.36	101.38	100.69
Wo	45	46	46	44	45	45	39	43	46	44	44	43
En	44	42	47	43	42	41	54	44	44	42	50	45
Fs	11	12	7	13	13	15	7	13	10	14	7	12

Unit[1]	Fakos												
Sample	LM50	LM50	LM50	LM50	LM50	LM50	LM50	LM50	LM45	LM45	LM45	LM45	LM45
Analysis no.*	48a	48b	48c	48d	49a+	49b+	49c+	49d+	50a+	50b+	50c+	50d+	50e+
SiO_2	51.68	51.66	53.07	51.97	52.64	50.30	51.60	50.61	52.88	54.29	52.47	54.17	52.89
TiO_2	0.28	0.25	0.26	0.23	0.38	0.51	0.41	0.54	0.28	0.32	0.42	0.38	0.30
Al_2O_3	1.54	1.52	0.65	1.25	1.01	2.45	2.01	2.67	1.51	0.88	1.81	1.03	1.44
Cr_2O_3	b.d.	b.d.	b.d.	0.01	0.07	b.d.	0.21	0.03	b.d.	0.23	b.d.	1.02	b.d.
FeO_t	7.79	8.62	4.81	7.69	4.51	8.57	4.74	7.13	8.43	4.84	7.83	4.00	7.85
MnO	0.43	0.53	0.16	0.50	0.13	0.43	0.11	0.29	0.47	0.14	0.28	0.15	0.43
MgO	14.68	14.41	17.43	15.07	17.47	14.19	16.66	14.94	15.16	17.95	15.55	17.77	15.15
CaO	23.17	22.99	23.57	23.10	23.50	22.49	24.05	23.23	21.76	22.24	22.17	22.55	22.23
Na_2O	0.52	0.64	0.20	0.45	0.23	0.66	0.33	0.43	0.44	0.18	0.35	0.29	0.44
Total	100.10	100.61	100.15	100.27	99.93	99.60	100.13	99.87	100.93	101.07	100.87	101.37	100.74
Wo	47	46	46	46	46	46	47	47	44	44	44	45	45
En	41	40	47	42	47	40	46	42	43	49	43	49	43
Fs	12	14	7	12	7	14	7	11	13	7	12	6	12

+refer to back-scattered electron image in Fig. 10.
b.d. = below detection limit.

*analyses listed in the form a-d refer to a transect from core to rim as shown here:

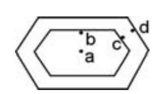

Table 7 Electron microprobe analyses of amphibole grains from selected samples of representative Limnos volcanic rocks.

Unit	Katalakon											
Mineral[1]	Mga-Has-Hbl	Mga-Has-Hbl	Mga-Has-Hbl	Mga-Has-Hbl	Mg-Has-Hbl	Mg-Has-Hbl	Mg-Has-Hbl	Mg-Has-Hbl	Mga-Has	Mg-Has	Mg-Has-Hbl	Mg-Has-Hbl
Sample	LM40	LM40	LM40	LM40	LM40	LM40	LM40	LM40	LM43	LM43	LM43	LM43
Analysis no.*	51a	51b	51c	51d	52a+	52b+	52c+	52d+	54a	54b	54c	54d
SiO_2	42.22	42.86	42.79	43.00	44.21	44.67	43.15	43.61	41.37	42.76	43.86	44.04
TiO_2	2.24	2.42	2.22	2.28	1.69	1.83	2.13	2.15	3.09	2.93	2.10	1.98
Al_2O_3	10.45	10.87	10.73	10.79	10.72	10.39	11.40	10.84	12.79	12.20	10.76	10.11
Cr_2O_3	b.d.	b.d.	b.d.	b.d.	b.d.	b.d.	b.d.	0.01	0.03	0.04	0.05	0.04
FeO_t	18.44	13.63	13.89	13.88	13.82	11.66	14.08	12.05	13.26	11.11	14.08	13.78
MnO	0.52	0.31	0.27	0.29	0.24	0.17	0.24	0.17	0.30	0.22	0.35	0.39
CaO	10.32	13.23	13.22	13.20	13.93	15.39	13.26	14.68	12.97	15.00	13.48	13.72
MgO	11.43	11.48	11.57	11.62	10.90	11.38	11.45	11.71	11.82	12.11	11.75	11.62
Na_2O	1.87	2.08	2.09	2.03	1.93	2.01	1.94	1.98	2.38	2.28	1.92	2.04
K_2O	1.09	0.84	0.85	0.92	0.96	0.86	0.84	1.10	0.91	0.99	0.72	0.72
Total	98.57	97.72	97.63	98.01	98.39	98.36	98.50	98.29	98.92	99.64	99.06	98.44

Unit	Myrina				Agios Ioannis					Fakos		
Mineral[1]	Mg-Hbl	Mg-Has	Edenite-Hbl	Edenite-Hbl	Edenite	Mga-Has	Edenite-Hbl	Edenite-Hbl	Mg-Has	Actinolite	Actinolite	Actinolite
Sample	LM65B	LM65B	LM61	LM61	LM13	LM13	LM13	LM13	LM07	LM50	LM45	LM45
Analysis no.*	55	56	62core	62rim	58	59	60core	60rim	61	63	64	66
SiO_2	46.60	41.22	46.13	45.82	47.21	41.33	44.89	45.03	42.22	53.18	55.63	55.92
TiO_2	1.17	3.09	1.90	1.76	1.65	2.70	1.59	1.55	2.62	0.32	0.25	0.11
Al_2O_3	7.21	11.54	9.26	8.47	9.13	13.56	9.09	9.00	12.21	2.15	1.71	1.32
Cr_2O_3	0.06	0.07	0.02	0.05	0.08	0.10	0.08	0.10	0.47	0.01	b.d.	b.d.
FeO_t	15.48	12.61	11.44	15.06	14.58	13.20	17.43	17.68	11.74	8.95	7.52	8.26
MnO	0.62	0.19	0.31	0.51	0.51	0.27	0.56	0.55	0.33	0.60	0.35	0.44
CaO	13.53	13.83	14.97	13.32	11.79	13.01	11.60	11.53	14.95	18.46	19.54	19.16
MgO	11.43	11.44	11.88	11.70	11.34	11.82	11.44	11.46	11.79	12.75	12.20	12.57
Na_2O	1.47	2.13	2.34	2.21	1.74	2.28	1.70	1.74	2.44	0.46	0.74	0.54
K_2O	0.78	1.48	0.93	0.93	1.06	1.20	1.17	1.14	1.03	0.10	0.12	0.03
Total	98.36	97.60	99.19	99.82	99.11	99.46	99.55	99.78	99.80	96.96	98.05	98.36

[1]Mineral abbreviations: Has, hastingsite; Hbl, hornblende; Mg, magnesio-; Mga, magnesian.
*analyses listed in the form a-d refer to a transect from core to rim as shown here:

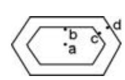

+refer to back-scattered electron image in Fig 10.
b.d. = below detection limit.

Table 8 Electron microprobe analyses of biotite grains from selected samples of representative Limnos volcanic rocks.

Unit[1]	Romanou						Katalakon (north)			Katalakon (south)		Fakos		Agios Ioannis		Myrina
Sample	LM31	LM31	LM24	LM25	LM22	LM22	LM40	LM43	LM43	LM72	LM72	LM50	LM45	LM15	LM15	LM65B
Analysis no.	73	75	77	78	79	80	70	71	72	67	69	86	87	83	84	81
SiO_2	35.89	38.39	36.37	37.40	36.53	36.99	37.73	36.96	37.38	36.33	36.23	36.97	38.27	37.68	36.14	36.21
TiO_2	5.50	5.51	5.66	7.08	5.42	5.07	4.22	5.35	5.57	5.61	5.25	5.48	5.81	4.86	5.01	4.36
Al_2O_3	16.74	13.53	14.49	14.90	13.98	14.09	14.00	14.42	14.67	14.68	14.03	14.12	13.53	15.91	14.75	13.21
Cr_2O_3	0.02	b.d.	0.01	0.04	0.03	0.02	b.d.	0.04	0.02	0.03	0.08	b.d.	b.d.	b.d.	b.d.	0.09
FeO_t	12.86	12.16	7.34	7.91	13.40	13.60	15.36	11.45	9.63	13.48	17.68	11.88	13.36	12.44	12.60	17.90
MnO	0.15	0.14	0.10	0.07	0.20	0.20	0.22	0.07	0.07	0.14	0.31	0.10	0.20	0.13	0.11	0.38
MgO	16.13	17.47	19.30	19.46	15.92	16.09	15.71	17.97	19.13	16.09	12.66	17.08	16.32	15.23	16.43	13.64
CaO	0.03	0.01	0.07	0.04	0.03	0.02	0.05	0.05	0.02	b.d.	0.02	b.d.	b.d.	1.11	0.04	0.02
Na_2O	0.72	0.77	0.59	0.75	0.52	0.60	0.54	0.48	0.45	0.68	0.40	0.58	0.60	0.43	0.54	0.54
K_2O	9.49	9.25	9.17	9.16	9.52	9.44	8.82	8.99	9.50	8.70	9.58	9.22	9.43	8.60	8.98	9.31
NiO	0.56	0.54	1.32	b.d.	0.08	0.06	0.47	b.d.	0.02	0.02	0.02	0.02	0.74	b.d.	b.d.	0.66
BaO	b.d.	0.01	b.d.	1.54	1.23	0.94	b.d.	0.87	0.73	1.53	0.39	0.81	0.04	1.03	0.86	0.05
Total	98.11	97.80	94.42	98.34	96.86	97.12	97.11	96.64	97.18	97.31	96.65	96.27	98.29	97.44	95.46	96.37

b.d. = below detection limit.

Table 9 Electron microprobe analyses of magnetite from selected samples of representative Limnos volcanic rocks

Unit[1]	Romanou		Katalakon (south)		Katalakon (north)		Fakos		Agios Ioannis		
Sample	LM25	LM25	LM72	LM72	LM43	LM43	LM50	LM50	LM15	LM15	LM07
Analysis no.	93	94	89	90	91	92	98	99	95	96	97
SiO_2	0.09	b.d.	b.d.	b.d.	b.d.	b.d.	b.d.	b.d.	0.37	0.03	0.73
TiO_2	13.11	10.06	6.12	6.85	3.44	2.17	6.91	6.32	5.23	3.48	3.11
Al_2O_3	0.64	1.07	1.67	2.61	2.83	1.03	0.65	0.32	0.45	1.12	1.01
Cr_2O_3	0.30	0.33	0.61	0.53	0.29	0.30	0.38	0.39	0.24	0.24	0.66
FeO_t	78.96	81.18	82.16	80.99	86.48	90.53	85.57	86.70	87.55	88.55	85.81
MnO	0.30	0.27	0.83	0.24	0.73	0.49	1.51	1.36	0.68	0.78	0.59
MgO	1.33	1.50	0.69	0.22	1.86	0.86	0.18	0.16	0.05	1.28	0.25
CaO	0.16	0.09	0.08	0.07	0.07	0.09	0.08	0.07	0.15	0.07	0.27
Total[^]	94.89	94.50	92.15	91.50	95.69	95.47	95.28	95.32	94.71	95.55	92.44

b.d. = below detection limit.

Table 4 Petrographical characteristics of analysed samples

Sample	Latititude	Longitude	Unit[1]	Field Occurrence	Rock Name[2]	Texture	Degree of alteration[3]	Phenocrysts & microphenocrysts[4]	Groundmass	Remarks, alteration products
LM02	39.96	25.11	KN	sill, 20 cm from top	dacite	porphyritic; spherulitic	high	feld$^+$; idiom amph$^+$; ?bi; ?px	hyalopilitic	Alt: cc; op; chl; act; ser; ms. Cavities filled with cc+ap.
LM06	39.97	25.08	KN	stock (intrusion)	trachyte	porphyritic	high	feld$^+$; amph$^+$; ?bi	hyalopilitic	Alt: cc; op; chl; act; ser; ms; ep. Small spherules of qtz±cc±chl±ep.
LM07	39.94	25.05	AI	?	trachydacite	porphyritic	med	plag; bi$^+$; idiom amph$^+$; K-feld; qtz	hyalopilitic	Alt: op; chl; hem; ?ep. Plag mgxt with growth twins; plag+qtz ph embayed; Spherules of qtz±chl.
LM11	39.93	25.06	AI	?	trachyte	porphyritic	high	plag; amph$^+$; bi; K-feld; qtz; ?px	hyalopilitic	Hydrothermal alt: chl; op; ser. Qtz ph embayed. Amph±?px replaced by qtz+chl+ser+op.
LM13	39.92	25.07	AI	?lava dome	trachyandesite	porphyritic	med	plag; idiom amph; bi; K-feld	hyalopilitic	Alt: cc; op; chl. Bi ph show flow texture. Plag ph embayed; some plag ph with idiom overgrowths. Cognate enclave of amph+plag+op. Small spherules of qtz±chl and cc veinlets. Glomerophyric clots of plag± interstitial glass.
LM14	39.92	25.07	AI	dyke in dacite	rhyolite	porphyritic	med	plag; K-feld; qtz; amph; bi;	hyalopilitic	Alt: op. Few bi ph show flow texture. Plag, qtz, K-feld ph fragmented and embayed.
LM15	39.92	25.14	AI	?	trachyte	porphyritic	med	plag; idiom bi; idiom amph; K-feld; rare qtz	hyalopilitic	Alt: op; chl. Spherules of qtz. Qtz ph rounded.
LM18	39.85	25.32	R	lava breccia	trachyte	porphyritic	high	plag; K-feld; px; biotite; amph	hyalopilitic	Alt: amph, biotite, and px altering to op. Plagioclase altering to chl.
LM24	39.88	25.31	R	lava	trachyte	porphyritic	med	plag; idiom px$^+$; bi$^+$; amph$^+$; rare K-feld	hyalopilitic w/ small patches alt brn glass	Alt: op; chl; clays.
LM25	39.88	25.31	R	intrusion in ?lava dome	trachyte	porphyritic	med	plag; idiom cpx; idiom bi; idiom amph; rare K-feld	hyalopilitic w/ small patches alt brn glass	Alt: op; chl; clays; ser. Cognate enclaves of feld+bi+cpx+interstitial glass.
LM28	39.91	25.29	R	lava breccia	trachyandesite	porphyritic	low	cpx; plag; bi; K-feld	hyalopilitic	Alt: op. Plag ph embayed. Zoning in cpx common. Cognate enclaves of cpx+plag+bi+op.
LM30	39.92	25.3	R	clast in conglomerate	trachyandesite	porphyritic	low	cpx; plag; bi; rare K-feld	hyalopilitic; largely dusty brown glass	Plag ph embayed. Zoning in cpx common. Cognate enclave of cpx+op+bi+plag.
LM31	39.92	25.3	R	clast in conglomerate	trachyandesite	porphyritic	low	cpx; plag; bi; rare K-feld	hyalopilitic; largely dusty brown glass	Plag ph embayed. Zoning in cpx common. Cognate enclaves of plag+cpx+bi+op and bi+plag+op.
LM32	39.92	25.3	R	clast in conglomerate	trachyandesite	porphyritic	low	cpx; plag; bi	hyalopilitic; largely dusty brown glass	Plag ph embayed. Zoning in cpx common.
LM35	39.94	25.15	KN	?lava	dacite	porphyritic	high	plag; ?px; ?amph; ?K-feld	hyalopilitic	Alt: chl; ep; op; ser.
LM39	39.95	25.16	KN	?lava	dacite	porphyritic; spherulitic	high	plag; bi; idiom amph$^+$	hyalopilitic	Alt: hem; op; chl; act; ep; clays. Spherules containing qtz (+spherulites).
LM40	39.95	25.17	KN	dyke	dacite	porphyritic; spherulitic	low	plag; idiom amph; bi	hyalopilitic	Alt: op; clays. Bi ph show flow texture. Plag ph embayed. Small cavities filled with qtz+ap; 3 crystals idiom allanite.
LM41	39.95	39.95	KN	?stock (intrusion)	dacite	porphyritic	high	feld$^+$; idiom amph$^+$; px$^+$; bi$^+$	hyalopilitic	Alt: cc; chl; op; ser; ep; clays. Spherules of qtz.
LM43	39.96	25.16	KN	dyke	dacite	porphyritic	med	plag; amph; bi	hyalopilitic	Alt: op; cc; ser; clays. Plag ph embayed. Very small spherules of qtz.
LM44	39.94	25.14	KN	float of intrusion	dacite	porphyritic	med	plag; K-feld; amph; biotite	hyalopilitic	Alt: amph altering to op.
LM45	39.81	25.17	F	(intrusion)	trachyte	porphyritic	high	plag; ?K-feld; cpx; bi	hyalopilitic	Alt: op; chl; cc; act; ep. Plag ph embayed. Cavities containing ep±act±chl±qtz. Cognate enclave of cpx+chl+act+ep+op.
LM48	39.82	25.17	F	dyke	trachyte	interlocking crystals	med	major minerals: plag; K-feld; qtz; amph; cpx; bi	N/A	Alt: chl; op. Medium-grained, inequigranular, interlocking texture.
LM50	39.82	25.17	F	dyke	trachyandesite	porphyritic	med	idiom cpx; plag; bi; rare qtz	hyalopilitic	Plag+qtz ph embayed. Cognate enclaves of cpx(alt)+plag+qtz+op and bi+op+plag.
LM53	39.92	25.08	M	lava dome	trachydacite	porphyritic	med	plag; K-feld; bi; rare idiom amph	trachytic	Alt: op; cc; chl; ep. Spherules of qtz+chl±cc. Idiom overgrowths of feld on subhedral plag; also plag ph embayed. Cognate enclave of plag+op+chl+cc.
LM54	39.92	25.08	M	lava dome	trachyte	porphyritic	high	plag; K-feld; qtz; biotite	trachytic	Alt: plag altering to cc. Biotite altering to op.
LM57	39.92	25.08	M	lava dome	trachydacite	porphyritic	med	plag; K-feld; bi; rare qtz; ?amph	hyalopilitic	Alt: hem; op; clays. Spherules of qtz±op±chl. Qtz ph embayed. Vein of dusty vfn qtz+glass+op. Idiom feld overgrowths on subhedral plag laths.

Table 4 Petrographical characteristics of analysed samples

Sample	Latititude	Longitude	Unit[1]	Field Occurrence	Rock Name[2]	Texture	Degree of alteration[3]	Phenocrysts & microphenocrysts[4]	Groundmass	Remarks, alteration products
LM58	39.92	25.08	M	lava dome	trachyte	porphyritic	med	plag; K-feld; bi; ?amph;	hyalopilitic	Alt: op; cc; chl; clays. Spherules of qtz+chl±cc. Idiom plag overgrowths on plag phenocrysts (subhedral to idiom).
LM61	39.85	25.07	M	lava flow	trachydacite	porphyritic	med	plag; qtz; idiom amph; bi; rare cpx	hyalopilitic w/ small patches alt brn glass	Alt: op. Glass incl in plag ph; cumulophyric plag. Qtz is rounded and embayed.
LM64	39.85	25.07	M	?lava dome	trachyte	porphyritic	med	plag; bi; idiom amph; qtz	hyalopilitic w/ small patches alt brn glass	Alt: op. Few idiom cpx mph. Qtz+plag ph embayed. Few zoned amph grains.
LM66	39.86	25.17	R	block in polymictic breccia	trachyte	porphyritic	med	plag; bi; idiom amph[+]; qtz; cpx, K-feld	hyalopilitic	Alt: op. Plag commonly embayed.
LM69	39.86	25.17	KS	lava	andesite	porphyritic	high	plag; cpx; biotite; amph	hyalopilitic	Alt: plag altering to cc. Biotite altering to op.
LM70B	39.87	25.18	R	lava breccia	trachyandesite	porphyritic	med	plag; biotite	hyalopilitic	Alt: biotite slightly altering to op.
LM72	39.9	25.17	KS	margin of dyke or stock	trachyandesite	porphyritic	med	plag; bi; idiom amph[+]; K-feld; qtz	hyalopilitic	Alt: op; cc; chl. Plag+qtz ph embayed. Cognate enclave of bi+amph(alt)+op+ glass. Small cavities filled with cc±qtz.
LM77	39.85	25.07	M	mxtic lava breccia	trachyte	porphyritic	high	K-feld; plag; amph; biotite	hyalopilitic	Alt: biotite and amph altering to op.
LM85	39.88	25.27	KS	lava dome	trachyandesite	porphyritic	med	plag; biotite; qtz; biotite	hyalopilitic	Alt: amph altering to cc and op. Biotite altering to cc and clay minerals.

[1]AI = Agios Ioannis; F = Fakos; M = Myrina; KN = Katalakon (north); KS = Katalakon (south); R = Romanou; [2]Rock nomenclature according to IUGS classification system (LeBas et al., 1986).
[3]Degree of alteration is a comparative assessmentof alteration in the studied rocks; [4]Phenocrysts and microphenocrysts are listed in order of decreasing abundance; [+]identified by crystal habit and form;
Abbreviations: act, actinolite; alt, altered/alteration; amph, amphibole; ap, apatite; bi, biotite; brn, brown; cc, calcite; chl, chlorite; cpx, clinopyroxene; ep, epidote; feld, feldspar; hem, hematite; idiom, idiomorphic;
incl, inclusion; K-feld, K-feldspar; mgxt, megacryst; mph, microphenocryst; ms, muscovite; op, opaque oxide minerals; ph, phenocryst; plag, plagioclase; px, pyroxene; qtz, quartz;
ser, sericite; sm, small; vfn, very fine-grained.

Table 5: Electron microprobe analyses of volcanic glasses

Rock Type[1]	Tra		Raft in Ignimbrite									
Sample	LM32-105	LM32-106	LM33-1	LM33-2	LM33-3	LM33-4	LM33-5	LM33-6	LM33-7	LM33-8	LM33-9	LM33-10
Major element oxides and select trace elements (wt %)												
SiO_2	68.57	69.31	64.83	65.46	65.10	64.93	65.10	65.43	65.40	64.70	64.89	65.19
TiO_2	0.64	0.61	0.29	0.30	0.33	0.34	0.32	0.36	0.34	0.35	0.32	0.34
Al_2O_3	14.54	14.38	14.69	14.56	14.71	14.44	14.80	14.84	14.81	14.62	14.57	14.56
FeO_t	2.36	2.33	1.76	1.46	1.57	1.77	1.63	1.06	1.14	1.95	2.15	1.55
MnO	0.21	0.22	0.04	0	0.02	0.04	0.04	b.d.	0.02	0.05	0.02	0.01
MgO	0.58	0.59	0.52	0.32	0.47	0.54	0.58	0.45	0.40	0.50	0.43	0.44
CaO	1.36	1.39	1.89	1.29	1.80	1.63	1.86	1.66	1.54	1.58	1.57	1.54
Na_2O	1.64	1.48	2.48	2.58	2.30	2.33	3.00	2.49	2.93	2.65	3.05	3.21
K_2O	6.83	6.91	7.65	6.52	7.50	7.48	6.74	7.41	6.85	6.96	6.71	7.00
P_2O_5	0.13	0.12	b.d.	b.d.	b.d.	b.d.	b.d.	b.d.	b.d.	b.d.	b.d.	b.d.
BaO	0.20	0.22	0.24	0.21	0.18	0.19	0.23	0.22	0.21	0.17	0.20	0.19
SrO	b.d.[2]	b.d.	0.12	0.10	0.10	0.14	0.09	0.04	0.08	0.10	0.11	0.14
Cl	b.d.	b.d.	0.11	0.10	0.06	0.06	0.10	0.11	0.11	0.11	0.09	0.13
Total	97.06	97.56	94.63	92.91	94.14	93.86	94.49	94.07	93.84	93.74	94.13	94.30
Rock Type	IgnR	Trd	Ignimbrite									
Sample	LM33-12	LM61-107	LM84-1	LM84-2	LM84-3	LM84-4	LM84-5	LM84-7	LM84-8	LM84-9	LM84-10	LM84-11
Major element oxides and select trace elements (wt %)												
SiO_2	65.70	67.91	66.96	65.47	66.36	67.20	67.11	66.90	66.78	65.54	66.65	67.16
TiO_2	0.31	b.d.	0.34	0.30	0.31	0.31	0.34	0.33	0.23	0.30	0.30	0.33
Al_2O_3	14.71	16.93	15.53	15.31	15.68	15.28	15.59	15.69	15.53	15.19	15.28	15.13
FeO_t	1.47	0.46	0.98	1.93	1.18	0.60	0.87	0.39	0.53	1.88	0.44	0.30
MnO	0.04	b.d.	0.03	0.05	0.05	0.05	0.04	0.02	0.03	0.06	0.01	0.03
MgO	0.35	b.d.	0.38	0.51	0.29	0.14	0.15	0.05	0.15	0.48	0.08	0.01
CaO	1.32	0.12	1.24	1.69	1.12	0.68	0.68	0.71	0.81	1.77	0.67	0.59
Na_2O	3.46	3.20	3.24	2.90	2.42	2.55	2.50	2.17	2.45	2.51	2.21	3.18
K_2O	6.80	11.19	6.91	6.93	7.08	7.46	7.58	7.45	7.37	6.97	7.60	7.46
P_2O_5	b.d.	b.d.	b.d.	b.d.	b.d.	b.d.	b.d.	b.d.	b.d.	b.d.	b.d.	b.d.
BaO	0.15	b.d.	0.21	0.09	0.22	0.13	0.16	0.19	0.18	0.22	0.27	0.20
SrO	0.06	b.d.	0.03	0.01	0.03	0.02	0.05	0.05	0.05	0.06	0.12	0.11
Cl	0.12	b.d.	0.06	0.05	0.10	0.11	0.09	0.10	0.10	0.10	0.11	0.10
Total	94.48	99.81	95.91	95.24	94.85	94.53	95.15	94.05	94.22	95.09	93.75	94.61

[1] Tra = trachyandesite clast in conglomerate (glass from a mineral clot); IgnR = raft in ignimbrite; Trd = trachydacite glass inclusion in plagioclase

[2] b.d. = below detection limit

Table 6 Electron microprobe analyses of clinopyroxene grains from selected samples of representative volcanic rocks.

Unit[1]	Romanou											
Sample	LM31	LM31	LM31	LM31	LM31	LM31	LM31	LM31	LM31	LM31	LM31	LM31
Analysis no.*	40a[+]	40b[+]	40c[+]	40d[+]	42a[+]	42b[+]	42c[+]	42d[+]	43a	43b	43c	43d
SiO_2	53.54	52.20	54.02	53.15	53.19	52.80	54.87	51.82	53.98	52.94	54.12	53.01
TiO_2	0.40	0.60	0.49	0.32	0.30	0.34	0.18	0.62	0.06	0.31	0.27	0.34
Al_2O_3	1.59	2.65	1.40	1.47	1.44	1.97	1.20	2.89	1.80	1.60	1.39	1.63
Cr_2O_3	0.01	0.03	0.04	0.03	0.03	0.01	0.60	b.d.	0.06	0.02	0.81	0.02
FeO_t	7.06	7.80	4.78	8.17	8.42	9.12	4.69	8.28	6.24	8.94	4.22	7.72
MnO	0.29	0.33	0.14	0.53	0.53	0.49	0.15	0.35	0.34	0.50	0.14	0.43
MgO	16.05	14.85	17.22	15.44	14.78	14.21	19.73	15.70	15.81	14.68	18.13	15.78
CaO	22.38	22.49	23.28	21.61	22.21	21.81	19.84	21.05	23.17	21.73	21.98	21.32
Na_2O	0.40	0.54	0.25	0.54	0.55	0.69	0.29	0.45	0.47	0.65	0.33	0.43
Total[^]	101.72	101.49	101.63	101.26	101.45	101.43	101.56	101.15	101.93	101.36	101.38	100.69
Wo	45	46	46	44	45	45	39	43	46	44	44	43
En	44	42	47	43	42	41	54	44	44	42	50	45
Fs	11	12	7	13	13	15	7	13	10	14	7	12

Unit[1]	Fakos												
Sample	LM50	LM50	LM50	LM50	LM50	LM50	LM50	LM50	LM45	LM45	LM45	LM45	LM45
Analysis no.*	48a	48b	48c	48d	49a[+]	49b[+]	49c[+]	49d[+]	50a[+]	50b[+]	50c[+]	50d[+]	50e[+]
SiO_2	51.68	51.66	53.07	51.97	52.64	50.30	51.60	50.61	52.88	54.29	52.47	54.17	52.89
TiO_2	0.28	0.25	0.26	0.23	0.38	0.51	0.41	0.54	0.28	0.32	0.42	0.38	0.30
Al_2O_3	1.54	1.52	0.65	1.25	1.01	2.45	2.01	2.67	1.51	0.88	1.81	1.03	1.44
Cr_2O_3	b.d.	b.d.	b.d.	0.01	0.07	b.d.	0.21	0.03	b.d.	0.23	b.d.	1.02	b.d.
FeO_t	7.79	8.62	4.81	7.69	4.51	8.57	4.74	7.13	8.43	4.84	7.83	4.00	7.85
MnO	0.43	0.53	0.16	0.50	0.13	0.43	0.11	0.29	0.47	0.14	0.28	0.15	0.43
MgO	14.68	14.41	17.43	15.07	17.47	14.19	16.66	14.94	15.16	17.95	15.55	17.77	15.15
CaO	23.17	22.99	23.57	23.10	23.50	22.49	24.05	23.23	21.76	22.24	22.17	22.55	22.23
Na_2O	0.52	0.64	0.20	0.45	0.23	0.66	0.33	0.43	0.44	0.18	0.35	0.29	0.44
Total	100.10	100.61	100.15	100.27	99.93	99.60	100.13	99.87	100.93	101.07	100.87	101.37	100.74
Wo	47	46	46	46	46	46	47	47	44	44	44	45	45
En	41	40	47	42	47	40	46	42	43	49	43	49	43
Fs	12	14	7	12	7	14	7	11	13	7	12	6	12

[+]refer to back-scattered electron image in Fig. 10.
b.d. = below detection limit.

*analyses listed in the form a-d refer to a transect from core to rim as shown here:

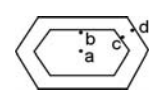

Table 7 Electron microprobe analyses of amphibole grains from selected samples of representative Limnos volcanic rocks.

Unit	Katalakon											
Mineral[1]	Mga-Has-Hbl	Mga-Has-Hbl	Mga-Has-Hbl	Mga-Has-Hbl	Mg-Has-Hbl	Mg-Has-Hbl	Mg-Has-Hbl	Mg-Has-Hbl	Mga-Has	Mg-Has	Mg-Has-Hbl	Mg-Has-Hbl
Sample	LM40	LM40	LM40	LM40	LM40	LM40	LM40	LM40	LM43	LM43	LM43	LM43
Analysis no.*	51a	51b	51c	51d	52a[+]	52b[+]	52c[+]	52d[+]	54a	54b	54c	54d
SiO_2	42.22	42.86	42.79	43.00	44.21	44.67	43.15	43.61	41.37	42.76	43.86	44.04
TiO_2	2.24	2.42	2.22	2.28	1.69	1.83	2.13	2.15	3.09	2.93	2.10	1.98
Al_2O_3	10.45	10.87	10.73	10.79	10.72	10.39	11.40	10.84	12.79	12.20	10.76	10.11
Cr_2O_3	b.d.	b.d.	b.d.	b.d.	b.d.	b.d.	b.d.	0.01	0.03	0.04	0.05	0.04
FeO_t	18.44	13.63	13.89	13.88	13.82	11.66	14.08	12.05	13.26	11.11	14.08	13.78
MnO	0.52	0.31	0.27	0.29	0.24	0.17	0.24	0.17	0.30	0.22	0.35	0.39
CaO	10.32	13.23	13.22	13.20	13.93	15.39	13.26	14.68	12.97	15.00	13.48	13.72
MgO	11.43	11.48	11.57	11.62	10.90	11.38	11.45	11.71	11.82	12.11	11.75	11.62
Na_2O	1.87	2.08	2.09	2.03	1.93	2.01	1.94	1.98	2.38	2.28	1.92	2.04
K_2O	1.09	0.84	0.85	0.92	0.96	0.86	0.84	1.10	0.91	0.99	0.72	0.72
Total	98.57	97.72	97.63	98.01	98.39	98.36	98.50	98.29	98.92	99.64	99.06	98.44

Unit	Myrina				Agios Ioannis					Fakos		
Mineral[1]	Mg-Hbl	Mg-Has	Edenite-Hbl	Edenite-Hbl	Edenite	Mga-Has	Edenite-Hbl	Edenite-Hbl	Mg-Has	Actinolite	Actinolite	Actinolite
Sample	LM65B	LM65B	LM61	LM61	LM13	LM13	LM13	LM13	LM07	LM50	LM45	LM45
Analysis no.*	55	56	62core	62rim	58	59	60core	60rim	61	63	64	66
SiO_2	46.60	41.22	46.13	45.82	47.21	41.33	44.89	45.03	42.22	53.18	55.63	55.92
TiO_2	1.17	3.09	1.90	1.76	1.65	2.70	1.59	1.55	2.62	0.32	0.25	0.11
Al_2O_3	7.21	11.54	9.26	8.47	9.13	13.56	9.09	9.00	12.21	2.15	1.71	1.32
Cr_2O_3	0.06	0.07	0.02	0.05	0.08	0.10	0.08	0.10	0.47	0.01	b.d.	b.d.
FeO_t	15.48	12.61	11.44	15.06	14.58	13.20	17.43	17.68	11.74	8.95	7.52	8.26
MnO	0.62	0.19	0.31	0.51	0.51	0.27	0.56	0.55	0.33	0.60	0.35	0.44
CaO	13.53	13.83	14.97	13.32	11.79	13.01	11.60	11.53	14.95	18.46	19.54	19.16
MgO	11.43	11.44	11.88	11.70	11.34	11.82	11.44	11.46	11.79	12.75	12.20	12.57
Na_2O	1.47	2.13	2.34	2.21	1.74	2.28	1.70	1.74	2.44	0.46	0.74	0.54
K_2O	0.78	1.48	0.93	0.93	1.06	1.20	1.17	1.14	1.03	0.10	0.12	0.03
Total	98.36	97.60	99.19	99.82	99.11	99.46	99.55	99.78	99.80	96.96	98.05	98.36

[1]Mineral abbreviations: Has, hastingsite; Hbl, hornblende; Mg, magnesio-; Mga, magnesian.
*analyses listed in the form a-d refer to a transect from core to rim as shown here:
[+]refer to back-scattered electron image in Fig 10.
b.d. = below detection limit.

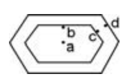

DR2008167

Table 8 Electron microprobe analyses of phlogopite - biotite grains from selected samples of representative Limnos volcanic rocks.

Unit[1]	Romanou						Katalakon (north)			Katalakon (south)		Fakos		Agios Ioannis		Myrina
Sample	LM31	LM31	LM24	LM25	LM22	LM22	LM40	LM43	LM43	LM72	LM72	LM50	LM45	LM15	LM15	LM65B
Analysis no.	73	75	77	78	79	80	70	71	72	67	69	86	87	83	84	81
Mineral	phlog.	phlog.	phlog.	phlog.	phlog.	phlog.	biot.	phlog.	phlog.	phlog.	biot.	phlog.	phlog.	phlog.	phlog.	biot.
SiO_2	35.89	38.39	36.37	37.40	36.53	36.99	37.73	36.96	37.38	36.33	36.23	36.97	38.27	37.68	36.14	36.21
TiO_2	5.50	5.51	5.66	7.08	5.42	5.07	4.22	5.35	5.57	5.61	5.25	5.48	5.81	4.86	5.01	4.36
Al_2O_3	16.74	13.53	14.49	14.90	13.98	14.09	14.00	14.42	14.67	14.68	14.03	14.12	13.53	15.91	14.75	13.21
Cr_2O_3	0.02	b.d.	0.01	0.04	0.03	0.02	b.d.	0.04	0.02	0.03	0.08	b.d.	b.d.	b.d.	b.d.	0.09
FeO_t	12.86	12.16	7.34	7.91	13.40	13.60	15.36	11.45	9.63	13.48	17.68	11.88	13.36	12.44	12.60	17.90
MnO	0.15	0.14	0.10	0.07	0.20	0.20	0.22	0.07	0.07	0.14	0.31	0.10	0.20	0.13	0.11	0.38
MgO	16.13	17.47	19.30	19.46	15.92	16.09	15.71	17.97	19.13	16.09	12.66	17.08	16.32	15.23	16.43	13.64
CaO	0.03	0.01	0.07	0.04	0.03	0.02	0.05	0.05	0.02	b.d.	0.02	b.d.	b.d.	1.11	0.04	0.02
Na_2O	0.72	0.77	0.59	0.75	0.52	0.60	0.54	0.48	0.45	0.68	0.40	0.58	0.60	0.43	0.54	0.54
K_2O	9.49	9.25	9.17	9.16	9.52	9.44	8.82	8.99	9.50	8.70	9.58	9.22	9.43	8.60	8.98	9.31
NiO	0.56	0.54	1.32	b.d.	0.08	0.06	0.47	b.d.	0.02	0.02	0.02	0.02	0.74	b.d.	b.d.	0.66
BaO	b.d.	0.01	b.d.	1.54	1.23	0.94	b.d.	0.87	0.73	1.53	0.39	0.81	0.04	1.03	0.86	0.05
Total	98.11	97.80	94.42	98.34	96.86	97.12	97.11	96.64	97.18	97.31	96.65	96.27	98.29	97.44	95.46	96.37

b.d. = below detection limit.

Table 9 Electron microprobe analyses of magnetite from selected samples of representative Limnos volcanic rocks

Unit[1]	Romanou		Katalakon (south)		Katalakon (north)		Fakos		Agios Ioannis		
Sample	LM25	LM25	LM72	LM72	LM43	LM43	LM50	LM50	LM15	LM15	LM07
Analysis no.	93	94	89	90	91	92	98	99	95	96	97
SiO_2	0.09	b.d.	b.d.	b.d.	b.d.	b.d.	b.d.	b.d.	0.37	0.03	0.73
TiO_2	13.11	10.06	6.12	6.85	3.44	2.17	6.91	6.32	5.23	3.48	3.11
Al_2O_3	0.64	1.07	1.67	2.61	2.83	1.03	0.65	0.32	0.45	1.12	1.01
Cr_2O_3	0.30	0.33	0.61	0.53	0.29	0.30	0.38	0.39	0.24	0.24	0.66
FeO_t	78.96	81.18	82.16	80.99	86.48	90.53	85.57	86.70	87.55	88.55	85.81
MnO	0.30	0.27	0.83	0.24	0.73	0.49	1.51	1.36	0.68	0.78	0.59
MgO	1.33	1.50	0.69	0.22	1.86	0.86	0.18	0.16	0.05	1.28	0.25
CaO	0.16	0.09	0.08	0.07	0.07	0.09	0.08	0.07	0.15	0.07	0.27
Total^	94.89	94.50	92.15	91.50	95.69	95.47	95.28	95.32	94.71	95.55	92.44

b.d. = below detection limit.